# Lithographically induced self-assembly of periodic polymer micropillar arrays

Stephen Y. Chou[a] and Lei Zhuang
*NanoStructure Laboratory, Department of Electrical Engineering, Princeton University, Princeton, New Jersey 08544*

(Received 18 June 1999; accepted 17 September 1999)

We observed, and believe it to be the first time, the self-formation of periodic, supramolecular (micrometer scale) pillar arrays in a thin, single-homopolymer film melt, which was originally flat on a plate. The self-formation was induced by placing a second plate (called a mask) *a distance above* the polymer film. The pillars, formed by rising against the gravitational force and surface tension, bridge the two plates. The pillar height is equal to the plate-mask separation, which is two to seven times the film's initial thickness. If the surface of the mask has a protruding pattern (e.g., a triangle or rectangle), the pillar array can be formed only under the protruding pattern with the edge of the array aligned to the boundary of the mask pattern. We also discuss a model and novel applications of lithographically induced self-assembly. © *1999 American Vacuum Society.* [S0734-211X(99)15206-5]

## I. INTRODUCTION

Self-assembly of periodic, polymer microstructures is of great importance to science and technology. Technologically, self-assembly promises not only low cost and high throughput, but also other advantages in patterning microstructures, which might be unavailable in conventional lithographies.

Previous studies of self-assembly have focused extensively on either phase separation of a polymer blend[1] or of diblock copolymers,[2] or of local modification of surface chemistry (i.e., chemical lithography).[3–5] In self-assembly by phase separation, the periodic structures are multidomain, and their orientation and locations are uncontrollable and random, making it nearly impossible to electrically contact each individual self-assembly structure for electronic device applications. A long-sought goal is to precisely control the orientation and location of a self-assembled polymer structure.

In chemical lithography, a lithographic mask is required, and the self-assembled patterns have the same lateral size as the patterns on the mask. Another long-sought goal is that if a mask is used to control a self-assembly, then the self-assembled structures should have a size that is smaller than that of the mask patterns.[6] This is also called the ''demagnification effect.'' If used repeatedly, it could achieve a size much smaller than that using a single self-assembly process.

In the process of investigating nanoimprint lithography (NIL),[7] we discovered a new self-assembly phenomenon from ''bad'' samples, where dust created a gap between the polymer and a NIL mask.[8] The new method, coined ''lithographically induced self-assembly'' (LISA), uses a mask to induce and control the self-assembly of periodic polymer pillar arrays. LISA offers a solution to the two long-sought goals mentioned above. In this article, we report detailed findings on the new method, present a model, and discuss possible applications.

[a]Electronic mail: chou@princeton.edu

## II. LISA PROCESS

In LISA, a smooth, thin, single-homopolymer film is first cast on a flat substrate. Then a mask with protruding patterns is placed above the film, but it is separated, using a spacer, from the film by a gap (Fig. 1).[8] The mask, the polymer film, and the substrate are heated uniformly to a temperature above the polymer's glass transition temperature, then are cooled down to room temperature. During the heat-cool cycle, the initially flat polymer film self-assembles into periodic supramolecular pillar arrays. The pillars, formed by rising against the gravitational force and surface tension, bridge the two plates. The pillar height is equal to the plate–mask separation. After pillar formation, due to a constant polymer volume, there is little polymer left in the area between the pillars. Moreover, if the surface of the mask has a protruding pattern (e.g., a triangle or rectangle), the pillar array can be formed only under the protruding pattern with the edge of the array aligned to the boundary of the mask pattern. The array's lattice structure is determined by the shape and size of the mask pattern. The location of each pillar can be precisely controlled by the patterns on the mask. In principle, the LISA process can be used repeatedly to further demagnify the self-assembled pattern size.

The polymer used in our LISA experiments is a homopolymer, polymethylmethacrylate (PMMA). Typically, the molecular weight and the film thickness of the PMMA are 2000 and 95 nm, respectively, and are not essential to LISA. A typical substrate is a silicon wafer with a thin layer of native oxide on its surface, making it a high energy surface and wet to a PMMA melt. A typical mask is also a silicon wafer with a monolayer surfactant on its surface, making it a low energy surface and dewet to a PMMA melt. The gap between the polymer film and the mask is about two to seven times that of the film's initial thickness. The protruding patterns on a mask are about 0.3 $\mu$m above the mask surface. Heating to 130 °C for 5–80 min was performed ei-

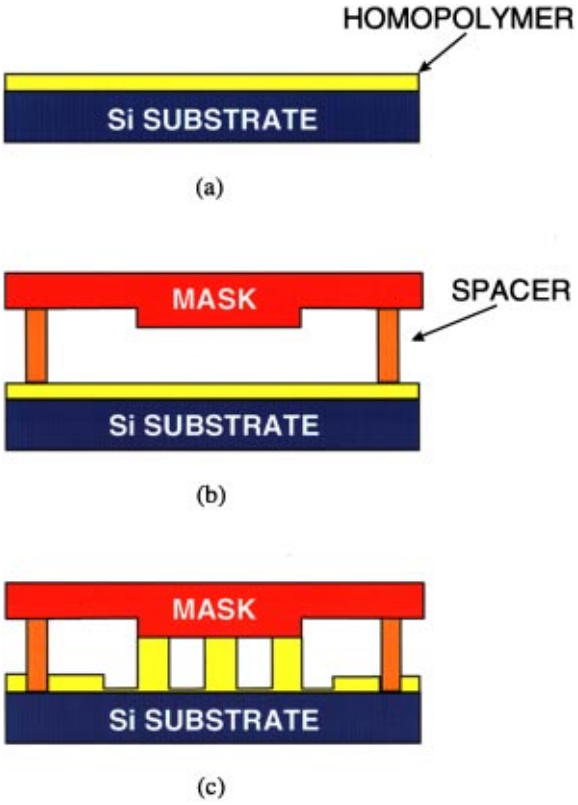


FIG. 1. Schematic of LISA: (a) a thin layer of PMMA spin coated on a flat silicon wafer. (b) A mask of protruding patterns placed a distance above the PMMA film, but separated by a spacer. (c) During a heat-cool cycle, the PMMA film self-assembled into a periodic supramolecular pillar array, with the location and lattice structure of the array controlled by the patterns on the mask.

ther in atmosphere or vacuum of 0.3 Torr, which had little effects on the results. A press was used to hold the substrate, the spacer, and the mask in their positions, hence keeping the mask–substrate separation constant.

## III. LISA EXPERIMENTAL RESULTS

Without a mask placed on top of the PMMA film, no patterns were observed in the polymer after the cool-heat cycle. However, if a mask is placed in the vicinity of PMMA film, the initially flat PMMA film can self-assemble into periodic pillar arrays.

For a mask without any protrusion (i.e., a plain flat surface) placed ~165 nm above the surface of the PMMA film, the original flat PMMA film became, after a heat-cool cycle, periodic PMMA pillar arrays with a close-packed hexagonal structure of 3.4 $\mu$m period, 2.7 $\mu$m pillar diameter, and 260 nm height (Fig. 2). The optical images showed that the pillar arrays were multidomain and over the entire sample. The average size of a single domain was about 50 $\mu$m (i.e., ~15 periods). Atomic force microscopy (AFM) showed that the top of each pillar was flat (due to contact with the mask) and the sidewall was quite vertical (note that the finite size of an AFM tip can make a sidewall appear sloped). A two-dimensional Fourier transform of the AFM images showed

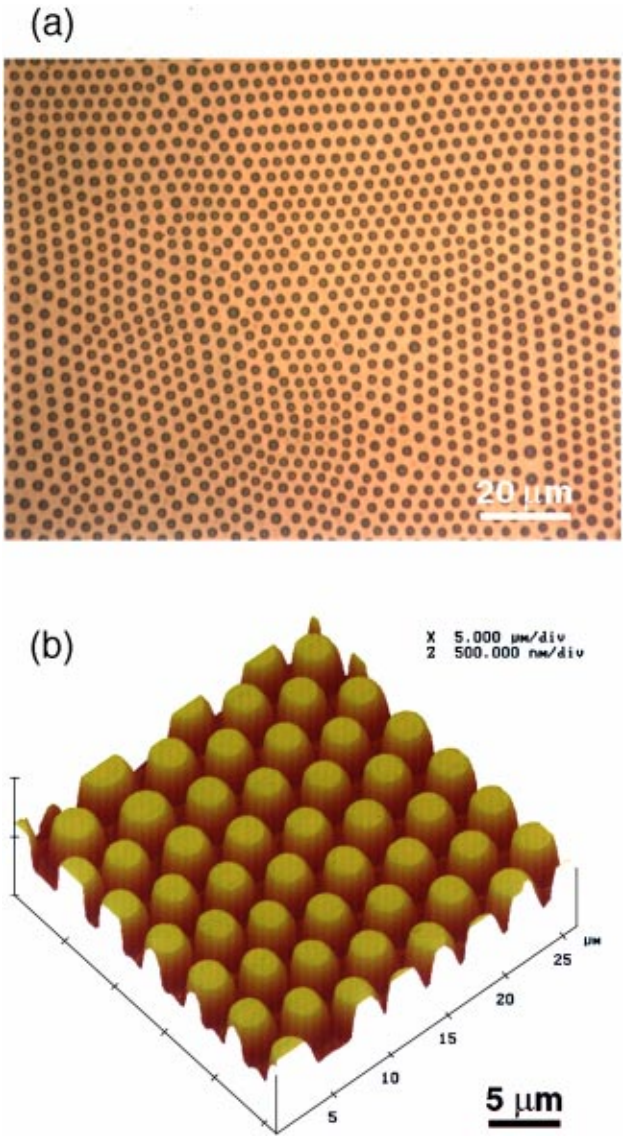


FIG. 2. (a) Optical and (b) AFM images of periodic PMMA pillars formed with LISA using a mask with a plain flat surface. The pillars, which have a close-packed hexagonal lattice and are multidomain, cover the entire wafer. A single domain is ~50 $\mu$m. The pillar period, diameter, and height are 3.4 $\mu$m, 2.7 $\mu$m, and 260 nm, respectively. The initial film thickness is 95 nm.

six sharp points arranged in a hexagonal shape in the *k* space, further confirming the hexagonal lattice structure of the pillars.

For a protruding triangle pattern on the mask of a 53 $\mu$m side, a single-domain, PMMA pillar array of a close-packed hexagonal lattice formed under the mask pattern (Fig. 3). Both optical and AFM images showed that the pillars on the edges of the array were aligned along the edges of the triangle mask pattern, making the boundary of the pillar array have the same shape and size as that of the mask pattern. No pillars were formed under the recessed areas of the mask. The separation between the substrate and the mask pattern (i.e., the pillar height) was 530 nm. The LISA pillar array had a periodicity of 3 $\mu$m and an average pillar diameter of 1.6 $\mu$m. For the triangle mask patterns with a side greater

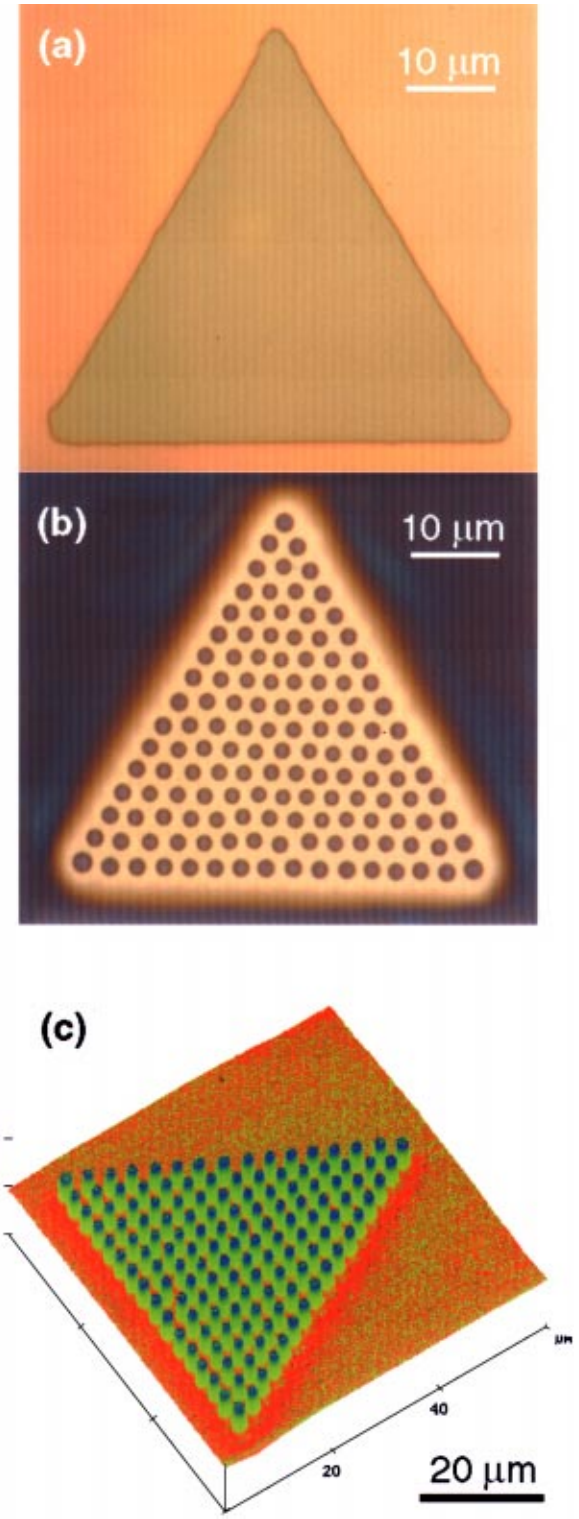


FIG. 3. Optical micrographs of (a) a protruding triangle pattern on the mask and (b) the LISA of the PMMA pillar array that formed under the triangle pattern. (c) AFM of the pillar array. The size and shape of the pillar array are identical to those of the mask pattern, with the pillars at the edges of the array aligned to the edges of the mask pattern. The pillars have a close-packed hexagonal structure with a 3 $\mu$m period, 1.6 $\mu$m pillar diameter, and 530 nm height (equal to the initial separation of the mask and substrate). The initial film thickness is 95 nm.

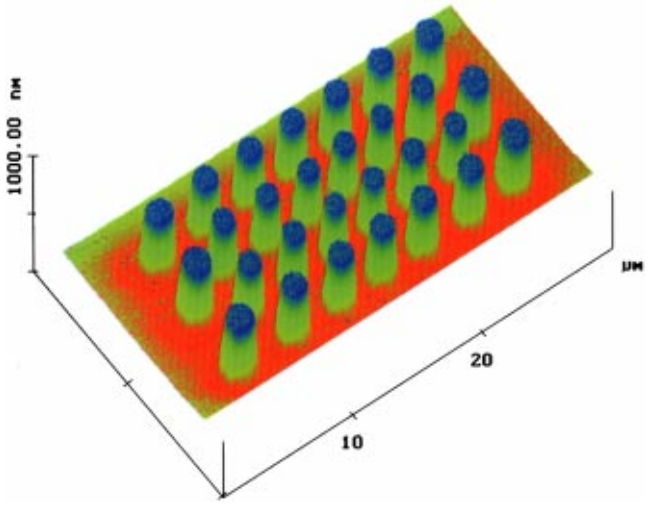


FIG. 4. AFM image of LISA of PMMA pillar arrays that formed under a protruding rectangular pattern. The pillar diameter, period, and height are 2 $\mu$m, 3.3 $\mu$m, and 440 nm, respectively.

than 53 $\mu$m, multidomain pillar arrays formed.

If the protruding patterns on the mask are rectangles or squares, the boundary of the pillar arrays formed in LISA also have a shape and size identical to the mask patterns, with the pillars at the edges of the array aligned to the edges of the mask patterns, just as in the case of the triangle mask pattern (Figs. 4 and 5). However, the lattice structures of the pillar arrays under the rectangle and square mask protrusion patterns were not hexagonal; they can be simple cubic, face centered, and other kinds, determined by the shape and size of the mask patterns and the separation between the protrusion and the PMMA film. Figures 5(b) and 5(c) show that the same mask pattern geometry but different mask–substrate separations lead to two different lattice structures. Moreover, the pillars at the edges have a diameter that is slightly larger than other pillars. Finally, if the mask pattern is a protruding line with a width less than 5 $\mu$m, a single line of pillars will form and be aligned under the line pattern (Fig. 6).

Further experimentation showed that the pillar diameter seems to decrease with increasing pillar height, and that the pillar period and size depend primarily on the polymer molecular weight. For example, for PMMA of 15 K molecular weight (made by a different vendor from 2 K PMMA), the pillar period and diameter became ~8 and ~5 $\mu$m, respectively. We also found that while the heating time varied from 5 to 80 min, the pillar period and diameter formed in LISA do not depend on the heating time. The highest ratio of the pillar height to the pillar diameter achieved is 0.5 (800 nm height and 1.6 $\mu$m diameter). Further study of the effects of polymers, substrates, masks, and processing conditions on the LISA patterns is in progress.

## IV. MODEL FOR LISA

LISA is very intriguing scientifically, because it cannot be explained by any existing models, such as phase separation or chemical lithography. Based on our further experimental and theoretical investigation, we have proposed a model for

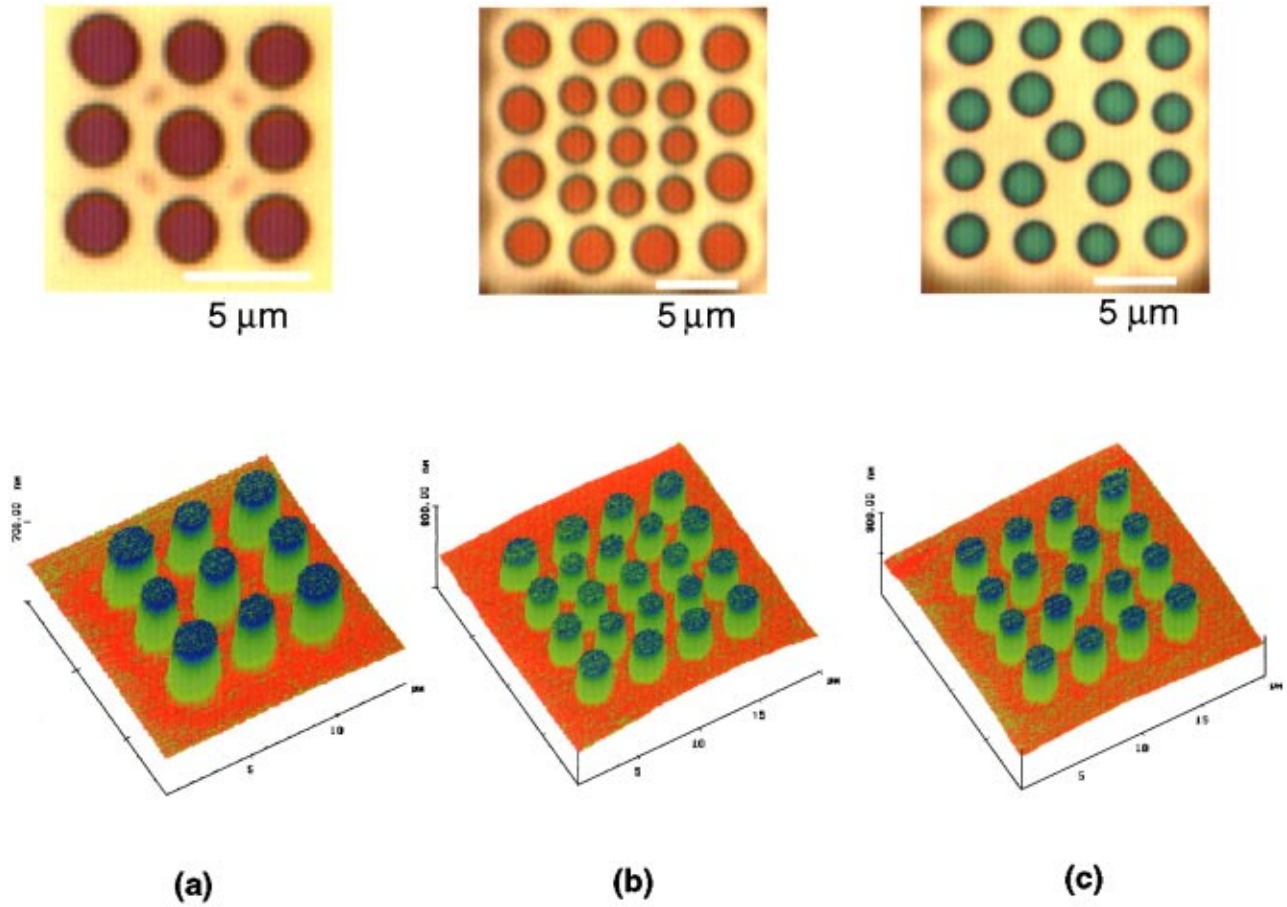


FIG. 5. Optical and AFM images of the LISA of PMMA pillar arrays that formed under protruding square patterns with sides of (a) 10, (b) 14, and (c) 14 $\mu$m. The separations between the mask and the substrate in (a)–(c) are 430, 280, and 360 nm, respectively.

LISA.[9] Although the details of the model and related experiments are beyond the scope of this article, we would like to summarize the key points of the model here.

The model, called the image charge-induced electrohydrodynamic-instability (ICE) model, assumes that electrostatic force is the driving force. The patterns are formed as a result of interplay and instability of charges in a polymer melt, image charges in a mask, and hydrodynamic force in the polymer melt. Our study showed that because the polymer melt thickness is ultrathin, LISA is not due to the instabilities from the thermal convection (Rayleigh–Benard instability[10]) or the surface tension driven Benard convention,[11] which also could lead to the pattern formation.

Some details of the ICE model are shown in Fig. 7. Upon heating PMMA above its glass transition temperature, it becomes a polymer melt, leading to a significant increase of both charge density and charge mobility in PMMA. If there is no mask placed on top of the PMMA melt, the charges in the PMMA film should be uniformly distributed due to a flat surface and symmetry. However, if there is a mask with finite conductivity placed near the PMMA melt, the image charge will be induced in the mask. The interplay of the charges and the image charges can cause instability and the formation of patterns.

Here we consider the case where the mask has a protruding square. Since the charges tend to accumulate at corners, there will be more image charges in the corners than other places on the protruding square, causing a nonuniform charge distribution in the mask. The nonuniform distribution of the image charge will cause redistribution of the charges in the PMMA film. The process continues in a positive feedback fashion. Eventually, enough charges and image charges


FIG. 6. (a) Optical micrograph of a protruding line pattern of the word ''PRINCETON'' on the mask and (b) AFM image of LISA of PMMA pillars that formed under the mask pattern.

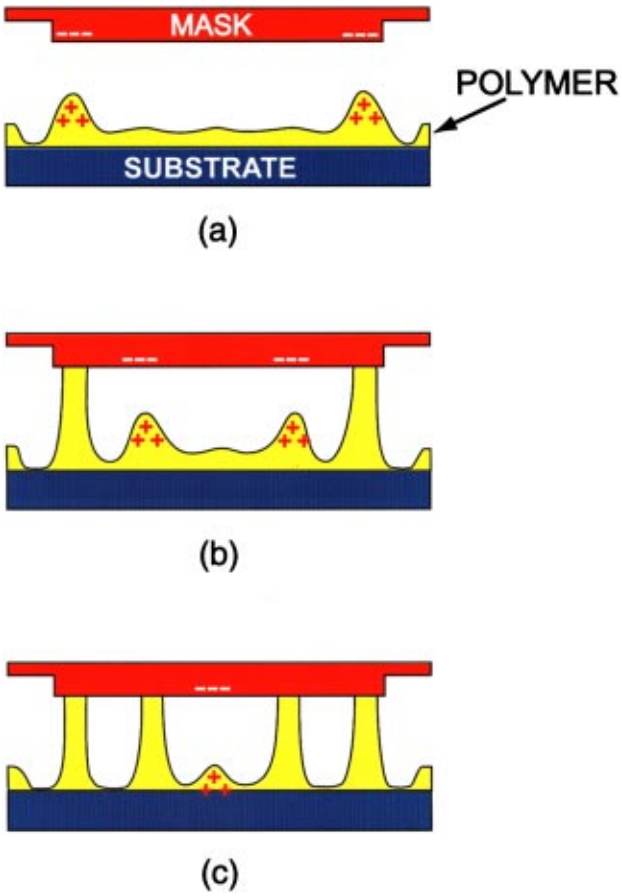


FIG. 7. ICE model for LISA suggesting three processes: (a) electrohydrodynamic (EHD) instability, due to the charge in PMMA and the image charges on the mask, make the PMMA melt under the corners of a mask rise. (b) Once the pillars at the corners are fully formed, they become the boundaries for the capillary waves in the PMMA melt. The EHD would then make the capillary wave peaks next to the boundary grow. (c) The process continues; the fully formed pillars formed at the corners first, then at the edges, and they later propagate to the center of the mask pattern.

will build up at the corners of the square mask pattern and in the PMMA areas under the corners, so that the electrostatic force between the corners of the mask patterns and the PMMA under the corners exceeds the gravitational force. The PMMA melt in those areas, which initially were flat, starts to be pulled up into smaller cones. The charge will move into the sharp point of the cones, hence inducing more image charges at the corners of the mask. If the mask is not too far from the PMMA, the charges and the image charges will build up a local electric field that can overcome the surface tension. In this case, the small PMMA cones will grow. The growth will reduce the distance between the charges and the image charges, hence increasing the strength of the electrostatic force and speeding up the growth. Finally the PMMA pillars reach the mask, forming a full pillar.

Once the full PMMA pillars are formed at the corners, the charges and image charges must redistribute. The pillars formed become a boundary for the capillary waves in the PMMA melt surface. The capillary wave, a linear wave of amplitude of about 1/100 of the film thickness (less than 1 nm in our case) will form standing waves set by the boundary. If the standing wave peak next to a boundary pillar has an amplitude that is slightly larger than the rest of the peaks, more charges will be accumulated in that peak and more images charges in the mask area above the peak, making the peak grow into a full pillar. Once the pillars reach the mask, the process will repeat, until all small amplitude capillary peaks under the mask protruding patterns develop into full pillars.

Therefore, the formation of the PMMA pillars starts at the corners, then at the edges, and later propagates into the center of the mask protruding pattern. On the other hand, the polymer under the recessed areas of the mask is too far away to have an electrostatic force to overcome surface tension and develop into full pillars.

## V. APPLICATION OF LISA

The LISA process opens up a new paradigm in patterning electronic and optoelectronic devices and circuits. Due to limited space here, we briefly describe several examples, the details of which will be published elsewhere.

The LISA process should, in principle, be applicable to other polymers and perhaps even to other single-phase materials, such as semiconductors, metals, and biological materials. The periodic arrays formed by LISA have many applications, such as memory devices, photonic materials, and new biological materials, just to name a few. With proper design, a single crystal lattice of a pillar array with predetermined diameter, period, location, and orientation could be achieved over an entire wafer.

With a suitable set of polymers of desired properties (e.g., viscosity, surface tension, etc.) and repeated usage of LISA, the diameter of the LISA pillars can be ''demagnified.'' [6]

With good control of the surface energy, polymer patterns with sizes identical to the patterns on masks can be formed [so-called lithographically induced self-construction (LISC)], rather than pillar arrays in a LISA.[12] LISC offers a unique way to pattern polymer electronic and optoelectronic devices directly without using the detrimental photolithography process.

A final example is a self-aligned self-assembly (SALSA) of random access electronic device arrays.[13] The conventional approach in fabricating such an array is to fabricate each individual device first, then connect them with word lines and bit lines. As the devices become smaller, the precision alignment between the wires and devices becomes more difficult to achieve, substantially increasing the fabrication cost. Using the LISA principle, we can first fabricate a word-line array and a bit-line array in two different substrates, and then let the device self-assemble between the word line and bit line.

## VI. CONCLUSION

We have discovered lithographically induced self-assembly that uses a mask to induce and control the self-assembly of periodic polymer pillar arrays. We proposed a model, called the image charge-induced electrohydrodynamic-instability model, that assumes that electrostatic

force is the driving force for LISA. The model is supported by experiments. LISA opens up new possibilities for further fundamental scientific study and practical applications. We have discussed a number of novel applications of LISA in making polymer electronic and optoelectronic device arrays.

## ACKNOWLEDGMENTS

The authors thank Steven Schablitski, Xiao-Yun Sun, and other members of NanoStructure Laboratory at Princeton University for their help in the experiments. The work was supported in part by DARPA and ONR.

[1]For a summary on phase separation of polymer blends, see, for example, J. D. Gunton, M. San Miguel, and P. Sahni, in *Phase Transition and Critical Phenomena*, edited by Domb Lebowitx (Academic, London, 1983), Vol. 8, pp. 267–466, and references therein.

[2]For a summary on phase separation of diblock copolymers, see, for example, F. S. Bates and G. H. Fredrickson, Annu. Rev. Phys. Chem. **41**, 525 (1990), and references therein.

[3]For a good summary on surface effects, see, for example, G. Krausch, Mater. Sci. Eng., R. **14**, 1 (1995), and references therein.

[4]J. C. Meiners, H. Elbs, A. Ritzi, J. Mlynek, and G. Krausch, J. Appl. Phys. **80**, 2224 (1996).

[5]M. Boltau, S. Walheim, J. Mlynek, G. Krausch, and U. Steiner, Nature (London) **391**, 877 (1998).

[6]S. Y. Chou (unpublished).

[7]S. Y. Chou, P. R. Krauss, and P. J. Renstrom, Appl. Phys. Lett. **67**, 3114 (1995); Science **272**, 85 (1996).

[8]S. Y. Chou and L. Zhuang (unpublished, 1997); Meeting of the American Physical Society, March 1999.

[9]S. Y. Chou, X. Y. Sun, and L. Zhuang (unpublished).

[10]R. Rayleigh, Philos. Mag. **32**, 529 (1916).

[11]H. Benard, Rev Gen. Sci. Pure Appl. **11**, 1261 (1900).

[12]S. Y. Chou, L. Zhuang, and L. J. Guo, Appl. Phys. Lett. **75**, 1004 (1999).

[13]S. Y. Chou, W. Wu, and L. Zhuang (unpublished).